



Adaptive tracking control of flapping wing micro-air vehicles with averaging theory

ISSN 2468-2322

Received on 5th January 2018

Revised on 12th February 2018

Accepted on 19th February 2018

doi: 10.1049/trit.2018.0007

www.ietdl.org

Chen Qian^{1,2}, Yongchun Fang^{1,2} ✉¹Institute of Robotics and Automatic Information Systems, College of Computer and Control Engineering, Tianjin 300353, People's Republic of China²Tianjin Key Laboratory of Intelligent Robotics, Nankai University, Tianjin 300353, People's Republic of China

✉ E-mail: fangyc@nankai.edu.cn

Abstract: An input constrained adaptive tracking controller is designed for flapping micro aerial vehicles, wherein the moving averaging filter is adopted to estimate the averaged states of the system. Specifically, in the outer loop controller, an observer is constructed to estimate the disturbances within the system. Moreover, the constrained thrust is designed to keep the frequency in a proper region so as to meet the requirement of average estimation. Then, a tracking differentiator is used to provide trackable trajectories for the inner loop. Subsequently, a new quaternion-based hybrid attitude tracking controller is designed which successfully deals with high-frequency noises and avoids possible chattering. As supported by mathematical analysis, the proposed control strategy guarantees the uniform ultimate boundedness of the closed-loop system, and it keeps the control torques within the permitted range to meet the application requirement. At last, numerical simulations are carried out to support the validity of the proposed controller, whose results are satisfactory even when the thrust and torques are saturated.

1 Introduction

In the size of insects and birds, flapping flight possesses amount of advantages [1, 2]. Based on this observation, many flapping wing micro vehicles have been invented till now, including *Mentor* flapping-wing micro air vehicle (FMAV) [3], *Delfly* [4], *Nano Hummingbird* [5], *Harvard Robotic Fly* [6] and so on. To make a flapping wing micro vehicle fly with much flexibility, it is of key importance to design and implement a suitable control for the system. In recent works, many control algorithms, such as model-free control [7], adaptive control [8, 9], geometric control [10], and some other control methods [11], have been successfully introduced for the control of different flapping wing vehicles.

In the past decade, the problem of stabilising the vehicle at the desired attitudes has long been a popular research topic for the control of flapping wing vehicles. Lin *et al.* use a modified P-control to stabilise the altitude of their *Golden Snitch* [12]. Banazadeh *et al.* design an adaptive sliding mode technique for the attitude and position control of a rigid body, insect-like flapping wing model in the presence of uncertainties [13]. An adaptive tracking controller is proposed in [14] for the Harvard fly. A common feature of these methods is that much effort has been focused on the attitude control of the studied FMAV. In fact, once the fast changing inner loop control (attitude control) is determined, the outer loop control (position control) can be designed according to practical applications with much flexibility. For the position control of an FMAV system [13, 14], averaging method proves to be a mainstream way to construct practical controllers [11, 15], which approximates the orbit of the oscillating system by the solution of an average system, resulting in more straightforward analysis for the system's stability [16]. Averaging theory seeks a way to approximate the non-autonomous vector field with an autonomous one. That is, with the help of averaging, one may use a non-linear time invariant system to describe the intractable non-linear time varying system [16]. The theory generally applies to numerous classes of time-dependent vector fields, instead of only strictly periodically varying vector fields [17]. More details about averaging theory could be found in [17, 18]. However, to utilise averaging method, the frequency of

the wing flap needs to be high enough and the flaps' effects need to be relatively stable. Another issue with averaging method is that the averaged vector field cannot be computed explicitly for an FMAV system in practical applications [16, 19]. In this paper, we seek no particular autonomous approximation. Oppositely, using a moving average filter, the original time-dependent vector field of FMAV is regarded as a non-autonomous vector field.

A main difficulty for flapping wing tracking is the unavoidable vibration, which is apparently reflected in the sense that both the forces and torques are oscillating. Also, practical flapping wing systems are intrinsically subjected to various input constraints. In fact, to facilitate the application of the averaging method, it is even necessary to set a lower bound on the flapping frequency. Therefore, how to propose a suitable controller to satisfy those constraints is another challenging issue. Considered the aforementioned problems and inspired by the work reported in [20, 21], this paper proposes an adaptive tracking control method for an FMAV system, which introduces averaged states as feedback signals and applies some robust auxiliary terms to handle the drifts or disturbances within the system. Meanwhile, considering that the measurement is always oscillating, the controller utilises the estimation generated from a reliable average estimator to construct the controller. To avoid singularity, some specific saturation function has been introduced and the quaternion-based description [22, 23] is adopted to construct attitude filters. The performance of the proposed adaptive tracking controller is verified by both rigorous analysis and simulation results.

The contribution of this paper mainly consists of the following three parts: (i) The proposed adaptive position tracking controller guarantees satisfactory control performance even in the presence of various disturbances and input constraints; (ii) a new quaternion-based attitude tracking controller is designed, which is free of singularity and successfully keeps the tracking error within a given bound; (iii) a systematic procedure is proposed, which designs control laws for the outer loop and the inner one separately, and thus brings much flexibility and increases the robustness of the overall system.

The main body of this paper falls into the following four sections: in Section 2, we briefly analyse the dynamics of the flapping wing

vehicle and provide the dynamic model of the system. Next, the control laws are designed in Section 3 in details. Stability analysis for the closed-loop system is performed in Section 4. Finally, some simulation results, with corresponding analysis, are presented in Section 5.

2 System dynamics analysis

It is worth stressing that flapping wings cause non-negligible transient effects on the vehicles' dynamics. For most practical designs, the vehicle's subcycle movement is neither controllable nor observable, and only macro parameters, for example, flapping frequency, can be adjusted relatively slowly. Parametrisation method is usually used to model the system, which conveniently sets up the relationship between the adjustable parameters and the forces/torques actuated on the vehicle. Later on, these parameters can be then regarded as control inputs to change the state of FMAVs. For example, Deng *et al.* use this method to parameterise the wing trajectory and then propose a flight controller for biomimetic robotic insects in [24].

Inspired by [24], also referring to [25], the dynamic equation for the studied FMAV system is given as

$$\frac{dX}{dt} = \frac{d}{dt} \begin{bmatrix} p \\ \dot{p} \\ q \\ {}^B \omega \end{bmatrix} = \begin{bmatrix} \dot{p} \\ g e_3 + {}^I_B R \frac{F_{ad}(X)}{m} \\ \frac{1}{2} q \otimes {}^B \omega \\ -J^{-1}({}^B \omega \times J {}^B \omega - \tau_{ad}(X)) \end{bmatrix} \quad (1)$$

$$+ \begin{bmatrix} 0 \\ q \otimes \frac{F_{th}}{m} \otimes q^* \\ 0 \\ J^{-1} \tau_r \end{bmatrix} + \begin{bmatrix} 0 \\ q \otimes \frac{F_p(t/\varepsilon, F_{th}, X)}{m} \otimes q^* \\ 0 \\ J^{-1} \tau_p(t/\varepsilon, F_{th}, \tau_r, X) \end{bmatrix}.$$

In (1), $X \in \mathbb{R}^{13}$ refers to the system states, including the position of the vehicle's mass centre $p \in \mathbb{R}^3$ in the inertia coordinate, the speed of the vehicle's mass centre $\dot{p} \in \mathbb{R}^3$ in the inertia coordinate, the unit quaternion $q \in \mathbb{Q}$ representing the attitude of the vehicle in the inertia coordinate and the angular rate ${}^B \omega \in \mathbb{R}^3$ in the body coordinate. The signal g represents gravitational acceleration, $e_3 = [0 \ 0 \ 1]^T$, m and J stand for the mass and the inertia matrix of the vehicle. ${}^I_B R \in \text{SO}(3)$ denotes the rotation from the vehicle body coordinate to the inertia coordinate, which can be calculated according to q . The definition of quaternion multiplication operator \otimes can be found in [23]. Steady aerodynamic damping force $F_{ad}(\cdot) \in \mathbb{R}^{13} \rightarrow \mathbb{R}^3$ and torque $\tau_{ad}(\cdot) \in \mathbb{R}^{13} \rightarrow \mathbb{R}^3$ depend on the states, which are parameterised as linear functions. Note that $F_p(t/\varepsilon, F_{th}, X) \in \mathbb{R} \times \mathbb{R}^3 \times \mathbb{R}^{13} \rightarrow \mathbb{R}^3$ and $\tau_p(t/\varepsilon, F_{th}, \tau_r, X) \in \mathbb{R} \times \mathbb{R}^3 \times \mathbb{R}^{13} \rightarrow \mathbb{R}^3$ determine the fast oscillating behaviours of the system, where ε denotes a small positive constant, and $F_{th} \in \mathbb{R}^3$, $\tau_r \in \mathbb{R}^3$ represent the normalised thrust input and torque input, respectively. In addition, F_p and τ_p are zero mean periodic functions if F_{th} , τ_r and X are stationary.

Assumption 1: Bounded actuation torque τ_r is supposed to be uniformly omnidirectionally adjustable around the origin, provided that F_{th} remains higher than a certain magnitude. This assumption is actually reasonable since it only implies that the vehicle's attitude is locally controllable.

Remark 1: (averaging drift): If certain assumptions are satisfied, Lemma 4.3.1 in Chapter 4 of [18] presents that the drift between the averaged system and the original one can be offset by a time-varying function of the order $\mathcal{O}(\delta_1(\varepsilon)/(\varepsilon T))$ as $\varepsilon \rightarrow 0$. Although it is not practical to determine the exact form of the

offset, there do exist bounded choices of the offset which keep the performance of the two systems sufficiently close. In this sense, the offset can be regarded as a part of the disturbances, which will be then addressed in the subsequently designed adaptive tracking controller.

Remark 2: (Control inputs): Since the relationships between the parameters and the average effect of input thrust are assumed known, F_{th} and τ_r are directly taken as the inputs of the system, instead of the flapping frequencies and the rudders' steering angles.

Remark 3: (aerodynamic forces torques): The aerodynamic forces and torques are divided into three pairs: (i) the steady aerodynamic damping F_{ad} and τ_{ad} , (ii) the fast oscillating terms F_p and τ_p , (iii) the steady input thrust F_{th} and torque τ_r . The steady aerodynamics and control inputs present the same form in the following averaged systems, while the averaged effects of F_p and τ_p correspond to the drifts taken as components of disturbances.

3 Control strategy development

For the studied FMAV system, the structure of the closed-loop system is demonstrated in Fig. 1. As can be seen, the states are filtered by a moving average filter, which estimates the average of the oscillating states. The filtered states are then utilised by both the inner loop controller and the outer loop one to calculate proper input for the FMAV system, wherein the outer loop controller directly determines the thrust input, as well as the desired orientations q_d by integrating the yaw signal. Subsequently, the quaternion filter between the two controllers translates the desired orientations q_d to a smooth trackable attitude trajectory q_f . Thereafter, the constrained torque is produced by the inner loop controller, which enables the vehicle to track the generated trajectory. Along these lines, the control inputs F_{th} , τ_x , τ_y and τ_z vary slowly since the average estimated states are employed as feedbacks, even though the flapping wing vehicle actually vibrates with high frequency. In general, by virtue of the average estimation of the states and the averaging method applied to the system, the complicated FMAV tracking task can be split into the following two sub-tasks: (i) determining the proper thrust direction; (ii) efficiently adjusting the controller when the thrust is relatively far from the desired one, with the input constraints and system disturbances successfully addressed, both of which can be fulfilled by the subsequently designed control strategy.

3.1 Outer loop control design

After the first-order averaging and rewriting x_1 as p , and x_2 as \dot{p} , the state space representation of the outer loop dynamics becomes

$$\begin{cases} \dot{x}_1 = x_2, \\ \dot{x}_2 = g e_3 - {}^I_B R {}^B v_M \theta_a + u_t + d_T. \end{cases} \quad (2)$$

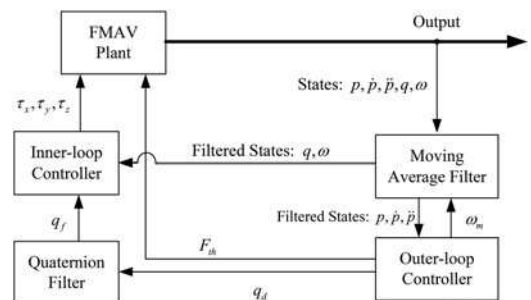


Fig. 1 Schematic diagram of the whole system

where the diagonal velocity matrix is defined as ${}^B\mathbf{v}_M = \text{diag}({}^Bv_x, {}^Bv_y, {}^Bv_z)$, $\boldsymbol{\theta}_a \in \mathbb{R}^3$ is the uncertain parameters vector of the translational normalised aerodynamic damping.

To keep the control torque effective and to satisfy the prerequisites of averaging method, it is necessary to set the upper and lower limits for the normalised thrust input $\mathbf{u}_t \in \mathbb{R}^3$ as $u_{t\min} \leq |\mathbf{u}_t| \leq u_{t\max}$, where $u_{t\min}$ and $u_{t\max}$ are both positive constants. Since the original oscillating states are replaced by the relatively steady averaged states, the drift of the averaged system or the estimation error will occur unavoidably. To deal with that, we use resultant force disturbance $\mathbf{d}_T \in \mathbb{R}^3$ to describe the deviation between slow varying part of the oscillating real system and the averaged system, which consists of three components, namely the averaged system drift, the averaging estimation error and the unknown disturbances (see also Remarks 1 and 3 for more details).

Assumption 2: In order to make the desired trajectory trackable, we assume that the trajectory, as well as its first and second derivatives, is continuous, bounded and known. Moreover, the desired yaw angle and its first and second derivatives are also assumed to be continuous, bounded and known. To facilitate subsequent description, we define the desired trajectory as \mathbf{x}_{1d} , and its derivative as \mathbf{x}_{2d} , and denote the tracking errors as $\mathbf{z}_1 = \mathbf{x}_1 - \mathbf{x}_{1d}$, $\mathbf{z}_2 = \mathbf{x}_2 - \mathbf{x}_{2d}$.

Assumption 3: As indicated by practical systems, the uncertain parameters vector $\boldsymbol{\theta}_a$ is bounded, in the sense that $\underline{\theta}_{aj} \leq \theta_{aj} \leq \bar{\theta}_{aj}$, for $0 < \underline{\theta}_{aj} < \bar{\theta}_{aj}$ with $j = x, y, z$.

Assumption 4: Without loss of much generality, the resultant force disturbance \mathbf{d}_T is assumed continuous and derivable. $\dot{\mathbf{d}}_T$ is assumed within a relatively small bound in the sense that $|\dot{\mathbf{d}}_T| \leq \sigma_{d_T}$, where $j = x, y, z$.

After some deep analysis for the system dynamics and referring to [21, 26], it is concluded that endowing the saturated controller with the robustness has the equivalent importance as using the dynamics model information and instant feedback does, thus, the control input is designed in the following manner:

$$\begin{aligned} \mathbf{u}_t &= \text{Sat}_T(\mathbf{u}_{t0}), \\ \mathbf{u}_{t0} &= -g\mathbf{e}_3 + {}^I_B \mathbf{R}^B \mathbf{v}_M \hat{\boldsymbol{\theta}}_a + \dot{\mathbf{x}}_{2d} - \boldsymbol{\eta} - \boldsymbol{\zeta} - \mathbf{K}_{z_2}^{-1} \mathbf{K}_{z_1} \mathbf{z}_2 \\ &\quad - (\mathbf{K}_{z_1} \mathbf{z}_1 + \mathbf{K}_{z_2} \mathbf{z}_2), \end{aligned} \quad (3)$$

with positive definite, diagonal matrices $\mathbf{K}_{z_1} \in \mathbb{R}^{3 \times 3}$ and $\mathbf{K}_{z_2} \in \mathbb{R}^{3 \times 3}$ as the control gains, where $\boldsymbol{\eta} \in \mathbb{R}^3$ and $\boldsymbol{\zeta} \in \mathbb{R}^3$ are both auxiliary terms for input constraint and system robustness, respectively. In (3), to ensure that the controller is always within the permitted range, the following three-dimensional saturation function $\text{Sat}_T(\cdot) \in \mathbb{R}^3 \rightarrow \mathbb{R}^3$ is constructed:

$$\text{Sat}_T(\mathbf{a}_T) = \begin{cases} {}^I_B \mathbf{R} \begin{bmatrix} 0 & 0 & u_{t\min} \end{bmatrix}^T, & |\mathbf{a}_T| \leq u_{ts}, \\ u_{t\min} \frac{\mathbf{a}_T}{\|\mathbf{a}_T\|}, & u_{ts} < |\mathbf{a}_T| \leq u_{t\min}, \\ \mathbf{a}_T, & u_{t\min} < |\mathbf{a}_T| \leq u_{t\max}, \\ u_{t\max} \frac{\mathbf{a}_T}{\|\mathbf{a}_T\|}, & |\mathbf{a}_T| > u_{t\max}, \end{cases} \quad (4)$$

where $\mathbf{a}_T \in \mathbb{R}^3$, u_{ts} , $u_{t\min}$ and $u_{t\max}$ are positive constants.

The update law of parameter estimation $\hat{\boldsymbol{\theta}}_a$ is designed as

$$\begin{aligned} \dot{\hat{\boldsymbol{\theta}}}_a &= \text{Proj}_{\hat{\boldsymbol{\theta}}_a} \left(-\Gamma_{\hat{\boldsymbol{\theta}}_a} {}^B\mathbf{v}_M {}^B\mathbf{R} \Gamma_{\hat{\boldsymbol{\theta}}_a}^{-1} \dot{\mathbf{d}}_T \right. \\ &\quad \left. + \Gamma_{\hat{\boldsymbol{\theta}}_a} {}^B\mathbf{v}_M {}^B\mathbf{R} \mathbf{K}_{z_2} (\mathbf{K}_{z_1} \mathbf{z}_1 + \mathbf{K}_{z_2} \mathbf{z}_2) - \Gamma_{\hat{\boldsymbol{\theta}}_a} \boldsymbol{\beta}_{\hat{\boldsymbol{\theta}}_a} \hat{\boldsymbol{\theta}}_a \right), \end{aligned} \quad (5)$$

where $\Gamma_{\hat{\boldsymbol{\theta}}_a} \in \mathbb{R}^{3 \times 3}$ and $\Gamma_{\boldsymbol{\theta}_a} \in \mathbb{R}^{3 \times 3}$ are positive definite, diagonal gain matrices, and the projection function, introduced to keep the estimates within the predefined range, is explicitly formulated as

$$\text{Proj}_{\hat{\boldsymbol{\theta}}_a}(\dot{\hat{\boldsymbol{\theta}}}_a) = \begin{cases} 0 & \text{if } \hat{\theta}_{aj} > \bar{\theta}_{aj} \text{ and } \dot{\hat{\theta}}_{aj} > 0 \\ 0 & \text{if } \hat{\theta}_{aj} < \underline{\theta}_{aj} \text{ and } \dot{\hat{\theta}}_{aj} < 0, \quad j = x, y, z. \\ \dot{\hat{\theta}}_{aj} & \text{otherwise} \end{cases} \quad (6)$$

Instead of directly tracking unobservable \mathbf{d}_T , it is convenient to track the modified observable variant \mathbf{d}_{temp} with compensation in other terms, since the deviation between \mathbf{d}_{temp} and \mathbf{d}_T is relative to the parameter estimation error. The specific observer for the resultant force disturbance \mathbf{d}_T is designed as

$$\begin{aligned} \dot{\mathbf{d}}_T &= -\Gamma_{\mathbf{d}_T} (\mathbf{K}_{\mathbf{d}_T} (\hat{\mathbf{d}}_T - \mathbf{d}_{\text{temp}}) + \mathbf{K}_{z_2} (\mathbf{K}_{z_1} \mathbf{z}_1 + \mathbf{K}_{z_2} \mathbf{z}_2)) \\ &\quad + \Gamma_{\mathbf{d}_T} \Xi_{\mathbf{d}_T} \boldsymbol{\sigma}_{\mathbf{d}_T}, \end{aligned} \quad (7)$$

where

$$\mathbf{d}_{\text{temp}} = \dot{\mathbf{x}}_2 - g\mathbf{e}_3 + {}^I_B \mathbf{R}^B \mathbf{v}_M \hat{\boldsymbol{\theta}}_\xi - \mathbf{u}_t, \quad (8)$$

and $\boldsymbol{\varepsilon}_\xi$ is a positive definite, diagonal matrix, and $\Xi_{\mathbf{d}_T}$ takes the form:

$$\begin{aligned} \Xi_{\mathbf{d}_T} &= \text{diag}(\xi_x, \xi_y, \xi_z), \\ \xi_i &= \tanh\left(\frac{d_{\text{temp}i} - \hat{d}_{Ti}}{\boldsymbol{\varepsilon}_{\xi i}}\right), \quad i = x, y, z. \end{aligned} \quad (9)$$

Note that the last term in (7), related with $\Xi_{\mathbf{d}_T}$, is introduced to cancel the intractable absolute term in the Lyapunov candidate derivatives, which will be shown in the subsequent stability analysis part.

The dynamic equation of the robust auxiliary term $\boldsymbol{\zeta}$ is defined as

$$\dot{\boldsymbol{\zeta}} = \boldsymbol{\varepsilon}_\xi^{-1} \mathbf{K}_{z_2} (\mathbf{K}_{z_1} \mathbf{z}_1 + \mathbf{K}_{z_2} \mathbf{z}_2) - \boldsymbol{\varepsilon}_\xi^{-1} \mathbf{K}_\xi (\boldsymbol{\zeta} - \hat{\mathbf{d}}_T), \quad (10)$$

where the gain matrix $\mathbf{K}_\xi \in \mathbb{R}^{3 \times 3}$ is positive definite and diagonal.

The update law for the auxiliary term $\boldsymbol{\eta}$ is designed to mitigate the influences caused by past time force constraints:

$$\dot{\boldsymbol{\eta}} = \begin{cases} -\mathbf{K}_\eta \boldsymbol{\eta} - \frac{1}{\|\boldsymbol{\eta}\|^2} (\mathbf{K}_{z_2} \|\mathbf{K}_{z_1} \mathbf{z}_1 + \mathbf{K}_{z_2} \mathbf{z}_2\| \cdot \|\Delta \mathbf{u}_t\|) \cdot \boldsymbol{\eta} \\ \quad + \mathbf{K}_{z_2} (\mathbf{K}_{z_1} \mathbf{z}_1 + \mathbf{K}_{z_2} \mathbf{z}_2), & \|\boldsymbol{\eta}\| > \sigma_\eta, \\ -\mathbf{K}_\eta \boldsymbol{\eta} - \frac{1}{\sigma_\eta^2} (\mathbf{K}_{z_2} \|\mathbf{K}_{z_1} \mathbf{z}_1 + \mathbf{K}_{z_2} \mathbf{z}_2\| \cdot \|\Delta \mathbf{u}_t\|) \cdot \boldsymbol{\eta} \\ \quad + \mathbf{K}_{z_2} (\mathbf{K}_{z_1} \mathbf{z}_1 + \mathbf{K}_{z_2} \mathbf{z}_2), & \|\boldsymbol{\eta}\| \leq \sigma_\eta, \end{cases} \quad (11)$$

where σ_η is a small positive constant, $\Delta \mathbf{u}_t = \text{Sat}_T(\mathbf{u}_{t0}) - \mathbf{u}_{t0}$, and $\mathbf{K}_\eta \in \mathbb{R}^{3 \times 3}$ is a positive definite, diagonal gain matrix.

The desired orientation \mathbf{q}_d is computed according to the thrust orientation $\mathbf{I}_t = \mathbf{u}_t / \|\mathbf{u}_t\|$ and the desired yaw angle ψ_d , with the specific method formulated as

$$\mathbf{q}_d = \mathbf{q}_\psi \otimes \frac{\mathbf{q}_{\text{raw}}}{\|\mathbf{q}_{\text{raw}}\|}, \quad (12)$$

$$\mathbf{q}_{\text{raw}} = [\mathbf{e}_3^T \mathbf{I}_t + \|\mathbf{I}_t\| \quad \mathbf{e}_3 \times \mathbf{I}_t], \quad (13)$$

where

$$\mathbf{q}_\psi = [\cos(\psi_d) \quad 0 \quad 0 \quad -\sin(\psi_d)]^T. \quad (14)$$

Remark 4: (Robustness enhancement): The term ξ detailed in (10) is seemingly redundant, yet it filters the higher frequency components of the observer $\hat{\mathbf{d}}_T$, which is mostly aroused by the term $\dot{\mathbf{x}}_2$ in \mathbf{d}_{temp} . Due to the existence of term $\varepsilon_\xi^{-1} \mathbf{K}_{z_2} (\mathbf{K}_{z_1} \mathbf{z}_1 + \mathbf{K}_{z_2} \mathbf{z}_2)$, ξ plays a similar role as the integration component in traditional PID control.

3.2 Inner loop control design

For inner loop control, the following quaternion-based hybrid filter is used to provide smooth attitude trajectory with the illumination of Mayhew's work [23], which relaxes the requirements on the desired trajectory stated in Assumption 1:

$$\begin{aligned} \dot{\mathbf{q}}_f &= \frac{1}{2} \mathbf{q}_f \otimes \boldsymbol{\omega}_f, \\ \boldsymbol{\omega}_{fd} &= \frac{1}{\delta_m (\|\mathbf{m}_{qd24}\|^2)} \left(-k_{qd} \mathbf{q}_d^T \mathbf{q}_f + \frac{k_{qd}}{\sigma_h(\mathbf{q}_d^T \mathbf{q}_f)} \right) \mathbf{m}_{qd24}, \end{aligned} \quad (15)$$

$$\dot{\boldsymbol{\omega}}_f = \mathbf{K}_{\omega_{fd}} (\boldsymbol{\omega}_{fd} - \boldsymbol{\omega}_f),$$

where $[m_{qd1} \ m_{qd2} \ m_{qd3} \ m_{qd4}]^T \triangleq \mathbf{M}^T(\mathbf{q}_f) \mathbf{q}_d$ and $\mathbf{m}_{qd24} \triangleq [m_{qd2} \ m_{qd3} \ m_{qd4}]^T$, with $\mathbf{M}(\cdot) \in \mathbb{Q} \rightarrow \mathbb{R}^{4 \times 4}$ denoting a matrix function of unit quaternion:

$$\mathbf{p} \otimes \mathbf{q} = \mathbf{M}(\mathbf{p}) \mathbf{q}, \quad (16)$$

$$\mathbf{p}^* \otimes \mathbf{q} = \mathbf{M}^T(\mathbf{p}) \mathbf{q}, \quad (17)$$

where \mathbf{p}^* stands for the conjugation of \mathbf{p} . In (15), k_{qd} is a positive constant and $\mathbf{K}_{\omega_{fd}}$ refers to a positive definite, diagonal matrix, $\sigma_h(\cdot)$ is a hysteretic function, which will be detailed below.

Based on the attitude dynamics (1) and Assumption 1, after using the first-order average and linearising the aerodynamic damping, the dynamics of ${}^B \boldsymbol{\omega}$ is calculated as

$$\begin{aligned} {}^B \dot{\boldsymbol{\omega}} &= g_T(\|\mathbf{u}_t\|) \mathbf{u}_\tau - {}^B \boldsymbol{\omega}_M \boldsymbol{\theta}_\tau \\ &\quad + {}^B \boldsymbol{\omega}_\times \boldsymbol{\theta}_{\tau \times} + \mathbf{d}_\tau, \end{aligned} \quad (18)$$

where the torque control gain $g_T(\cdot)$ is a known monotonously increasing function, and

$${}^B \boldsymbol{\omega}_M = \text{diag}({}^B \omega_x, {}^B \omega_y, {}^B \omega_z), \quad (19)$$

$${}^B \boldsymbol{\omega}_\times = \text{diag}({}^B \omega_x^B \omega_y, {}^B \omega_x^B \omega_z, {}^B \omega_y^B \omega_z), \quad (20)$$

$\boldsymbol{\theta}_\tau \in \mathbb{R}^3$ and $\boldsymbol{\theta}_{\tau \times} \in \mathbb{R}^3$ are uncertain parameters of the normalised damping and the normalised reduced inertia terms, and $\mathbf{d}_\tau \in \mathbb{R}^3$ is the total normalised torque disturbance. The inertia matrix is assumed to be diagonal, due to the reason that most FMAVs are designed symmetrical. Moreover, $\mathbf{u}_\tau \in \mathbb{R}^3$ stands for the normalised torque input.

Remark 5: (Torque control gain): In (18), the term $g_T(\|\mathbf{u}_t\|)$ is assumed to be known, while the damping and inertia terms are uncertain. For a practical system, this assumption is reasonable since the torque control gain $g_T(\|\mathbf{u}_t\|)$ can be obtained for a fixed platform, yet the damping and the inertia terms cannot be

determined conveniently as they are also influenced by various aerodynamic factors.

Assumption 5: For the studied system, the signals $\boldsymbol{\theta}_\tau$, $\boldsymbol{\theta}_{\tau \times}$ and \mathbf{d}_τ are assumed bounded as

$$0 < \underline{\theta}_{\tau aj} < \theta_{\tau aj} \leq \bar{\theta}_{\tau aj}, \quad (21)$$

$$|\theta_{\tau a \times j}| \leq \sigma_{\tau a \times j}, \quad (22)$$

$$|d_{\tau j}| \leq \sigma_{d \tau j}, \quad (23)$$

$$|\dot{d}_{\tau j}| \leq \sigma_{dd \tau j}, \quad (24)$$

where $j = x, y, z$.

With the motivation to obtain smooth desired angular rates, and to avoid unexpected effects of hybrid system jump, the compensation term \mathbf{q}_ξ is introduced with the inspiration of command filter [27], which is generated via the following manner:

$$\begin{aligned} \dot{\mathbf{q}}_\xi &= \frac{1}{2} \mathbf{q}_\xi \otimes \boldsymbol{\omega}_\xi, \\ \boldsymbol{\omega}_{\xi d} &= \frac{1}{\delta_m (\|\mathbf{q}_{\xi v}\|^2)} \left(k_{q_\xi} q_{\xi s} - \frac{k_{q_\xi}}{\sigma_h(q_{\xi s})} \right) \mathbf{q}_{\xi v}, \end{aligned} \quad (25)$$

$$\delta_m(a_m) = \begin{cases} a_m & \|a_m\| > \delta_{m0} \\ \delta_{m0} & \text{otherwise} \end{cases}$$

$$\dot{\boldsymbol{\omega}}_\xi = \mathbf{K}_{\omega_\xi} (\boldsymbol{\omega}_{\xi d} - \boldsymbol{\omega}_\xi) + \mathbf{K}_c (a_\omega - \boldsymbol{\omega}_d),$$

with the positive constant k_{q_ξ} and positive diagonal matrices $\mathbf{K}_{\omega_\xi} \in \mathbb{R}^{3 \times 3}$ and $\mathbf{K}_c \in \mathbb{R}^{3 \times 3}$ as the compensator gains. The term δ_{m0} refers to a small positive constant. Additionally, $q_{\xi s}$ and $\mathbf{q}_{\xi v}$ are the scalar and vectorial parts of quaternion \mathbf{q}_ξ .

It is important to avoid chattering occurring around the point $\mathbf{q}_f^T (\mathbf{q}_\xi \otimes \mathbf{q}) = 0$, because the real system is oscillating and prone to fall into the chattering range. Inspired by the hysteretic fashion presented in [23], the virtual angular speed a_ω is constructed as

$$\begin{aligned} a_\omega &= \frac{1}{\delta_m(\|\mathbf{m}_{qf}\|^2)} \left(-g_{qb} - g_{qf} \right) \mathbf{m}_{qf}, \\ g_{qb} &= k_q \mathbf{q}_f^T (\mathbf{q}_\xi \otimes \mathbf{q}) - \frac{k_q}{\sigma_h(\mathbf{q}_f^T (\mathbf{q}_\xi \otimes \mathbf{q}))}, \\ g_{qf} &= 2 \mathbf{q}_f^T (\mathbf{q}_\xi \otimes \mathbf{q}) + \mathbf{q}_f^T (\mathbf{q}_\xi \otimes \boldsymbol{\omega}_\xi \otimes \mathbf{q}). \end{aligned} \quad (26)$$

in which $[m_{qf1} \ m_{qf2} \ m_{qf3} \ m_{qf4}]^T \triangleq \mathbf{q}^* \otimes \mathbf{q}_\xi^* \otimes \mathbf{q}_f$, and $\mathbf{m}_{qf} \triangleq [m_{qf2} \ m_{qf3} \ m_{qf4}]^T$, and k_q , as a positive constant, denotes the virtual angular velocity control gain. The term $\sigma_h(a)$ is a one-dimensional hysteretic function as shown in Fig. 2, whose upper half and lower half are $\sigma_{h1}(a)$ and $\sigma_{h2}(a)$, respectively. The complete form of the function is shown as

$$\sigma_h(a) = \begin{cases} \sigma_{h1}(a), & \bar{c} = c_1, \\ \sigma_{h2}(a), & \bar{c} = c_2, \end{cases} \quad (27)$$

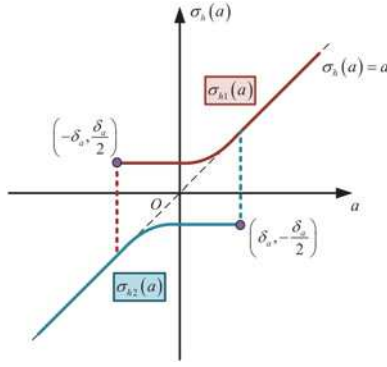


Fig. 2 Hysteretic function used in the virtual control law

where

$$\sigma_{h1}(a) = \begin{cases} \frac{\delta_a}{2}, & -\delta_a \leq a \leq 0, \\ \frac{a^2}{2\delta_a} + \frac{\delta_a}{2}, & 0 < a \leq \delta_a, \\ a, & \delta_a < a, \end{cases} \quad (28)$$

$$\sigma_{h2}(a) = \begin{cases} -\frac{\delta_a}{2}, & 0 < a \leq \delta_a, \\ -\frac{a^2}{2\delta_a} - \frac{\delta_a}{2}, & -\delta_a < a \leq 0, \\ a, & a \leq -\delta_a, \end{cases}$$

$$c(\bar{c}, a) = \begin{cases} c_1 & \text{if } \bar{c} = c_1 \text{ and } a > -\delta_a, \\ & \text{or } \bar{c} = c_2 \text{ and } a > \delta_a, \\ c_2 & \text{if } \bar{c} = c_1 \text{ and } a \leq -\delta_a, \\ & \text{or } \bar{c} = c_2 \text{ and } a \leq \delta_a. \end{cases}$$

Item c_i , $i = 1, 2$ is the function-choosing flag, introduced to identify which part of the hysteretic function the system is currently located on. \bar{c} is the flag c in last computing cycle. The positive constant δ_a determines the width of the flat area, which is clearly shown in Fig. 2.

As mentioned previously, we use a second-order filter to shield the negative effects aroused by the hybrid system jumps:

$$\begin{aligned} \dot{\omega}_d &= \varepsilon_{\omega n} \omega_{d1}, \\ \dot{\omega}_{d1} &= -2\xi_{\omega n} \varepsilon_{\omega n} \omega_{d1} - \varepsilon_{\omega n} (\omega_d - a_{\omega}). \end{aligned} \quad (29)$$

Similar as (3), the normalised torque is used to provide the control input with the specific composition formulated as

$$\begin{aligned} u_{\tau} &= \text{Sat}_{\tau}(u_{\tau 0}), \\ u_{\tau 0} &= \frac{1}{g_T(\|u_t\|)} (\dot{a}_{\omega} + {}^B \omega_M \hat{\theta}_{\tau a} - {}^B \omega_{\times} \hat{\theta}_{\tau \times} - \hat{d}_{\tau}) \\ &\quad - \frac{1}{2g_T(\|u_t\|)} \left(d\sigma_h(q_f^T(q_{\xi} \otimes q)) q_f^T(q_{\xi} \otimes q) \right. \\ &\quad \left. + \sigma_h(q_f^T(q_{\xi} \otimes q)) m_{qf} - \eta_{\tau} + \frac{1}{g_T(\|u_t\|)} (K_4(\omega_d - \omega)) \right), \end{aligned} \quad (30)$$

where the positive diagonal matrix $K_4 \in \mathbb{R}^{3 \times 3}$ denotes the control gain. Note that $d\sigma_h$ is the derivative of the function σ_{h1} with respect to a , if the flow is on the first continuous part. After the jump, the term $d\sigma_h$ becomes the derivative of σ_{h2} with respect to a . Thus, there is no infinitive point for the function $d\sigma_h$, even though the function σ presents two jumps. For practical reasons, the normalised torque constraint is considered, and the specific

saturation function $\text{Sat}_{\tau}(\cdot) \in \mathbb{R}^3 \rightarrow \mathbb{R}^3$ takes the following form:

$$\text{Sat}_{\tau}(v) = \begin{cases} -\sigma_{\tau i}, & v < -\sigma_{\tau i}, \\ v, & -\sigma_{\tau i} \leq v \leq \sigma_{\tau i}, \\ \sigma_{\tau i}, & v > \sigma_{\tau i}. \end{cases} \quad (31)$$

The update laws of the uncertain parameters are designed as

$$\dot{\hat{\theta}}_{\tau a} = \text{Proj}_{\theta_{\tau a}} (\Gamma_{\tau a} {}^B \omega_M (\omega_d - \omega) - \Gamma_{\tau a} \beta_{\tau a} \hat{\theta}_{\tau a}), \quad (32)$$

$$\dot{\hat{\theta}}_{\tau \times} = \text{Proj}_{\theta_{\tau \times}} (-\Gamma_{\tau \times} {}^B \omega_{\times} (\omega_d - \omega) - \Gamma_{\tau \times} \beta_{\tau \times} \hat{\theta}_{\tau \times}), \quad (33)$$

$$\dot{\hat{d}}_{\tau} = \text{Proj}_{d_{\tau}} (-\Gamma_{d_{\tau}} (\omega_d - \omega) - \Gamma_{d_{\tau}} \beta_{d_{\tau}} \hat{d}_{\tau}), \quad (34)$$

where $\beta_{\tau a}$, $\beta_{\tau \times}$, $\beta_{d_{\tau}}$, $\Gamma_{\tau a}$, $\Gamma_{\tau \times}$, and $\Gamma_{d_{\tau}}$, all belonging to $\mathbb{R}^{3 \times 3}$, are positive diagonal gain matrices, and the projection function follows the previous definition in (6) with bounds shown in Assumption 5. Note that every entry of $\beta_{d_{\tau}}$ should be larger than corresponding entry of $\Gamma_{d_{\tau}}^{-1}$, which enhances the convergence. The observer is not used for inner loop control because the direct angular acceleration is unobservable.

The term $\eta_{\tau} \in \mathbb{R}^3$ in (30) is used to alleviate the influences caused by past time constraint of normalised torque. Similar to (11), the update law of η_{τ} is constructed as

$$\dot{\eta}_{\tau} = \begin{cases} -k_{\eta_{\tau}} \eta_{\tau} - \left(\frac{g_T(\|u_t\|)}{\|\eta_{\tau}\|^2} \|\omega_d - \omega\| \cdot \|\Delta u_{\tau}\| \right) \cdot \eta_{\tau} & \|\eta_{\tau}\| > \sigma_{\eta_{\tau}}, \\ +g_T(\|u_t\|) \cdot (\omega_d - \omega), & \\ -k_{\eta_{\tau}} \eta_{\tau} - \left(\frac{g_T(\|u_t\|)}{\sigma_{\eta_{\tau}}^2} \|\omega_d - \omega\| \cdot \|\Delta u_{\tau}\| \right) \cdot \eta_{\tau} & \|\eta_{\tau}\| \leq \sigma_{\eta_{\tau}}, \\ +g_T(\|u_t\|) \cdot (\omega_d - \omega), & \end{cases} \quad (35)$$

where $\sigma_{\eta_{\tau}}$ is a small positive constant, $k_{\eta_{\tau}}$ refers to the positive gain and $\Delta u_{\tau} = \text{Sat}_{\tau}(u_{\tau 0}) - u_{\tau 0}$.

4 Stability analysis

This section presents the stability analysis for the proposed control strategy.

Theorem 1: For the flapping wing vehicle governed by (1), the control law given in (3), (4) and (30), together with the desired attitude (12), ensures that the tracking errors of the position and yaw angle are uniformly ultimately bounded.

Proof: For the sake of clarity, we will present the proof in two parts, namely for the inner loop controller and the outer loop one, respectively.

Analysis for the inner loop: To start with, as mentioned in (15), the filter translates the desired orientation to a continuous attitude trajectory as $q_f(t)$. Essentially, it is a generator for the desired trajectory. Therefore, it may be more comprehensible to treat the filter as a tracking differentiator of the signal q_d , rather than a part of the inner loop controller. The convergence of the filter can be verified in a similar method validating the convergence of (26).

In accordance with the virtual angular speed definition (26), choose the Lyapunov candidate for the first step as

$$V_q = 1 - \sigma_h(q_f^T(q_{\xi} \otimes q)) q_f^T(q_{\xi} \otimes q). \quad (36)$$

From (26) and (36), we know that V_q is positive when $q_f^T(q_{\xi} \otimes q) \notin \{-1, 1\}$, zero when $q_f^T(q_{\xi} \otimes q) \in \{-1, 1\}$, and V_q reaches its maximum right before its jump at $q_f^T(q_{\xi} \otimes q) = \delta_a$ or

$\mathbf{q}_f^T(\mathbf{q}_\xi \otimes \mathbf{q}) = -\delta_a$. Similar analysis is performed when $\|\mathbf{m}_{qf}\|^2 > \delta_{m0}$, otherwise, the actual attitude is in the neighbourhood of the desired attitude.

For the sake of brevity, we only present the analysis for the situations when the system locates on σ_{h1} as an illustrative example. Bearing the definition of the hysteretic function (27) and (28) in mind, the stability analysis for the system with the proposed virtual control input can be distributed into three parts. For $\mathbf{q}_f^T(\mathbf{q}_\xi \otimes \mathbf{q}) > \delta_a$

$$V_q = 1 - \left(\mathbf{q}_f^T(\mathbf{q}_\xi \otimes \mathbf{q})\right)^2, \quad (37)$$

whose derivative is

$$\dot{V}_q = -k_q \left(1 - \left(\mathbf{q}_f^T(\mathbf{q}_\xi \otimes \mathbf{q})\right)^2\right). \quad (38)$$

For $0 < \mathbf{q}_f^T(\mathbf{q}_\xi \otimes \mathbf{q}) \leq \delta_a$

$$V_q = 1 - \frac{\left(\mathbf{q}_f^T(\mathbf{q}_\xi \otimes \mathbf{q})\right)^3}{2\delta_a} - \frac{\delta_a}{2} \mathbf{q}_f^T(\mathbf{q}_\xi \otimes \mathbf{q}), \quad (39)$$

whose derivative can be calculated as

$$\begin{aligned} \dot{V}_q &= 3k_q \frac{\left(\mathbf{q}_f^T(\mathbf{q}_\xi \otimes \mathbf{q})\right)^3}{2\delta_a} + \frac{k_q \delta_a}{2} \mathbf{q}_f^T(\mathbf{q}_\xi \otimes \mathbf{q}) - 3k_q \\ &\quad + \frac{2k_q \delta_a^2}{\left(\mathbf{q}_f^T(\mathbf{q}_\xi \otimes \mathbf{q})\right)^2 + \delta_a^2} \leq 2k_q \left(\delta_a^2 - \frac{1}{2}\right), \end{aligned} \quad (40)$$

where the fact $\mathbf{q}_f^T(\mathbf{q}_\xi \otimes \mathbf{q}) \in [-1, 1]$ has been utilised. Choosing $\delta_a < (\sqrt{2}/2)$, then $\dot{V}_q < -C_{q2}$, with $C_{q2} = -2k_q(\delta_a^2 - (1/2))$. For $-\delta_a < \mathbf{q}_f^T(\mathbf{q}_\xi \otimes \mathbf{q}) \leq 0$

$$V_q = 1 - \frac{\delta_a}{2} \left(\mathbf{q}_f^T(\mathbf{q}_\xi \otimes \mathbf{q})\right), \quad (41)$$

its derivative can be obtained as

$$\dot{V}_q = -k_q \left(1 - \frac{\delta_a}{2} \left(\mathbf{q}_f^T(\mathbf{q}_\xi \otimes \mathbf{q})\right)\right). \quad (42)$$

In subsequent analysis, we will consider the jump effect on the system's convergency. Due to the symmetry of the hysteretic function, two jumps generate the same change of V_q , which is $\Delta V_q = -(3/2)\delta_a^2$. Therefore, V_q is decreasing even when the system goes through the discontinuous jumps. Owing to the filter, the jump effect does not appear explicitly in the following parts of the system. Consequently, there is no need to apply special analysis for the corresponding Lyapunov functions. Moreover, the analysis is similar with the former analysis when the system is on σ_{h2} , hence, it is omitted here. According to (40) and (42), it can be shown that V_q reaches the region $V_q < 1 - \delta_a^2$ in finite time $t < (\delta_a^2/2k_q) + (\delta_a^2/C_{q2})$ when the initial condition satisfies $\mathbf{q}_f^T(\mathbf{q}_\xi \otimes \mathbf{q}_0) \in (-\delta_a, \delta_a)$, and then, as indicated by (38), V_q converges to the region where $\|\mathbf{m}_{qf}\|^2 \leq \delta_{m0}$, exponentially fast, with adjustable bound δ_{m0} defined in (25). The bound δ_a can be selected to meet different robustness requirements, as long as it is smaller than $\sqrt{2}/2$.

Using the energy function as the Lyapunov candidate for the second part, we have

$$\begin{aligned} V_\omega &= \frac{1}{2}(\boldsymbol{\omega}_d - \boldsymbol{\omega})^T(\boldsymbol{\omega}_d - \boldsymbol{\omega}) + \frac{1}{2}\tilde{\boldsymbol{\theta}}_\tau^T \boldsymbol{\Gamma}_\tau^{-1} \tilde{\boldsymbol{\theta}}_\tau \\ &\quad + \frac{1}{2}\tilde{\boldsymbol{\theta}}_{\tau\times}^T \boldsymbol{\Gamma}_{\tau\times}^{-1} \tilde{\boldsymbol{\theta}}_{\tau\times} + \frac{1}{2}\tilde{\mathbf{d}}_\tau^T \boldsymbol{\Gamma}_{d\tau}^{-1} \tilde{\mathbf{d}}_\tau + \frac{1}{2}\boldsymbol{\eta}_\tau^T \boldsymbol{\eta}_\tau. \end{aligned} \quad (43)$$

The parameters estimation errors are defined as $\tilde{\boldsymbol{\theta}}_\tau = \hat{\boldsymbol{\theta}}_\tau - \boldsymbol{\theta}_\tau$, $\tilde{\boldsymbol{\theta}}_{\tau\times} = \hat{\boldsymbol{\theta}}_{\tau\times} - \boldsymbol{\theta}_{\tau\times}$ and $\tilde{\mathbf{d}}_\tau = \hat{\mathbf{d}}_\tau - \mathbf{d}_\tau$, respectively.

With the proposed update laws (32)–(35) and control laws (30) and (31), the derivative of (43) transforms into

$$\begin{aligned} \dot{V}_\omega &+ \frac{1}{2} \left(-d\sigma_h \left(\mathbf{q}_f^T(\mathbf{q}_\xi \otimes \mathbf{q}) \right) \mathbf{q}_f^T(\mathbf{q}_\xi \otimes \mathbf{q}) \right. \\ &\quad \left. - \sigma_h \left(\mathbf{q}_f^T(\mathbf{q}_\xi \otimes \mathbf{q}) \right) \right) \mathbf{m}_{qf24}^T (\boldsymbol{\omega} - \boldsymbol{\omega}_d) \\ &= -(\boldsymbol{\omega}_d - \boldsymbol{\omega})^T \mathbf{K}_4 (\boldsymbol{\omega}_d - \boldsymbol{\omega}) - \frac{1}{2} \tilde{\boldsymbol{\theta}}_\tau^T \boldsymbol{\beta}_\tau \tilde{\boldsymbol{\theta}}_\tau \\ &\quad - \frac{1}{2} \tilde{\boldsymbol{\theta}}_{\tau\times}^T \boldsymbol{\beta}_{\tau\times} \tilde{\boldsymbol{\theta}}_{\tau\times} - \frac{1}{2} \tilde{\mathbf{d}}_\tau^T (\boldsymbol{\beta}_{d\tau} - \boldsymbol{\Gamma}_{d\tau}^{-1}) \tilde{\mathbf{d}}_\tau - k_{\eta_\tau} \boldsymbol{\eta}_\tau^T \boldsymbol{\eta}_\tau \\ &\quad + \frac{1}{2} \tilde{\boldsymbol{\theta}}_\tau^T \boldsymbol{\beta}_\tau \boldsymbol{\theta}_\tau + \frac{1}{2} \tilde{\boldsymbol{\theta}}_{\tau\times}^T \boldsymbol{\beta}_{\tau\times} \boldsymbol{\theta}_{\tau\times} + \frac{1}{2} \tilde{\mathbf{d}}_\tau^T \boldsymbol{\beta}_{d\tau} \mathbf{d}_\tau \\ &\quad + \frac{1}{2} \boldsymbol{\sigma}_{dd\tau}^T \boldsymbol{\Gamma}_{d\tau}^{-1} \boldsymbol{\sigma}_{dd\tau}. \end{aligned} \quad (44)$$

The second term on the left side of (44) is the un-compensated part of last step. Based on previous analysis, we can conclude that $V_i = V_q + V_\omega$ is uniformly bounded when the system remains in a proper domain where $\|\mathbf{m}_{qf}\|^2 > \delta_{m0}$ and $\|\boldsymbol{\eta}_\tau\| > \sigma_{\eta_t}$ as described in (26) and (35). If $\|\mathbf{m}_{qf}\|^2 \leq \delta_{m0}$, then the attitude tracking error is relatively small. According to (35), because $\left((g_T(\|\mathbf{u}_t\|)) / \|\mathbf{h}_\tau\|^2 \right)$, $\left((g_T(\|\mathbf{u}_t\|)) / \sigma_{\eta_t}^2 \right)$ and $g_T(\|\mathbf{u}_t\|)$ are all positive, $\boldsymbol{\eta}_\tau$ keeps small in the region $\|\boldsymbol{\eta}_\tau\| \leq \sigma_{\eta_t}$, only when the angular velocity error $(\boldsymbol{\omega}_d - \boldsymbol{\omega})$ remains relatively small, since its derivative is bounded. In addition, $\boldsymbol{\omega}$ is bounded due to the damping term in (18), the bounded torque input and the bounded torque disturbance. Relatively small angular velocity error indicates that the virtual angular speed \mathbf{a}_ω can be obtained with tolerable small errors. Then, we treat the inner loop system as the following hybrid system to obtain thorough comprehension:

$$\mathcal{H} \begin{cases} \dot{\mathbf{x}} = F(\mathbf{x}, \mathbf{q}_f, \mathbf{d}_\tau), & \mathbf{x} \in C, \\ \mathbf{x}^+ \in G(\mathbf{x}), & \mathbf{x} \in D, \end{cases} \quad (45)$$

where $\mathbf{x} = \text{col}(\mathbf{q}_\xi, \mathbf{q}, \mathbf{a}_\omega, \boldsymbol{\omega}_d, \boldsymbol{\omega}_{d1}, \mathbf{u}_\tau, \hat{\boldsymbol{\theta}}_\tau, \hat{\boldsymbol{\theta}}_{\tau\times}, \hat{\mathbf{d}}_\tau, \hat{\boldsymbol{\eta}}_\tau)$, and most of the states have no dramatic change during the jump on account of the commander filter. The flow set and the jump set are defined according to the aforementioned hysteretic function:

$$\begin{aligned} C &= \left\{ \mathbf{x} \in \mathcal{X} : \sigma_h \left(\mathbf{q}_f^T(\mathbf{q}_\xi \otimes \mathbf{q}) \right) \mathbf{q}_f^T(\mathbf{q}_\xi \otimes \mathbf{q}) \geq -\frac{\delta_a^2}{2} \right\}, \\ D &= \left\{ \mathbf{x} \in \mathcal{X} : \sigma_h \left(\mathbf{q}_f^T(\mathbf{q}_\xi \otimes \mathbf{q}) \right) \mathbf{q}_f^T(\mathbf{q}_\xi \otimes \mathbf{q}) \leq -\frac{\delta_a^2}{2} \right\}. \end{aligned} \quad (46)$$

With the definition of the hybrid system and the choice of the closed sets, the system satisfies assumptions (A0)–(A3) in [28] with inspection. The conditions (VC) and (VD) in [28] are also satisfied accordingly, which ensure the existence of the hybrid system's solution. In this circumstance, \mathbf{q}_f is bounded and smooth enough to maintain the viability of the flow set. After checking the derivatives of the Lyapunov candidates, we can conclude that the

largest invariant set is included in

$$W = \left\{ \mathbf{x} \in \mathcal{X} : \|\mathbf{m}_{qf}\|^2 \leq \delta_{m0L}, \|\boldsymbol{\eta}_\tau\| \leq \sigma_{\eta L} \right\}, \quad (47)$$

where δ_{m0L} and $\sigma_{\eta L}$ are positive constants satisfying $\delta_{m0L} > \delta_{m0}$ and $\sigma_{\eta L} > \sigma_{\eta}$. Therefore, according to Corollary 7.7 in [28], the system asymptotically converges to the largest invariant set in W , implying that the attitude tracking error, including the yaw angle error, is uniformly ultimately bounded. In addition, the chattering problem analysis is similar with the one presented in [23], from which we know that the hysteretic function successfully inhibits the chattering at the unstable equilibrium point of $(\mathbf{q}_f^T(\mathbf{q}_\xi \otimes \mathbf{q})) = 0$.

Therefore, as long as the filter and the inner loop controller perform fast enough, and the initial orientation error is bounded, the orientation error will be uniformly bounded in any arbitrarily small bounds. This fact states that the virtual control forces are obtained instantly, and the unachieved part can be regarded as a part of force resultant disturbances. Although with different manners, this kind of cooperation problem between inner loop controller and outer loop one is also considered in [29, 30].

Analysis for the outer loop: After rigorous inner loop controller stability analysis, it is straightforward to analyse the stability of the outer loop controller.

Based on the outer loop controller design and the system characteristics, we choose the Lyapunov candidate as

$$\begin{aligned} V_o = & \frac{1}{2} (\mathbf{K}_{z_1} \mathbf{z}_1 + \mathbf{K}_{z_2} \mathbf{z}_2)^T (\mathbf{K}_{z_1} \mathbf{z}_1 + \mathbf{K}_{z_2} \mathbf{z}_2) + \frac{1}{2} \boldsymbol{\eta}^T \boldsymbol{\eta} \\ & + \frac{1}{2} \tilde{\boldsymbol{\theta}}_a^T \Gamma_{\theta a}^{-1} \tilde{\boldsymbol{\theta}}_a + \frac{1}{2} (\boldsymbol{\zeta} - \hat{\mathbf{d}}_T)^T \boldsymbol{\varepsilon}_\zeta (\boldsymbol{\zeta} - \hat{\mathbf{d}}_T) \\ & + \frac{1}{2} (\mathbf{d}_T - \hat{\mathbf{d}}_T)^T \Gamma_{d_T}^{-1} (\mathbf{d}_T - \hat{\mathbf{d}}_T). \end{aligned} \quad (48)$$

The coefficients $\boldsymbol{\varepsilon}_\zeta$, \mathbf{K}_{z_1} , \mathbf{K}_{z_2} , $\Gamma_{\theta a}$ and Γ_{d_T} are all positive definite, diagonal matrices. The variable \mathbf{d}_T is the disturbance observer, and the uncertain parameter estimation error is defined as $\tilde{\boldsymbol{\theta}}_a = \hat{\boldsymbol{\theta}}_a - \boldsymbol{\theta}_a$. Differentiating both sides of (48), the derivative of the Lyapunov candidate (48) is obtained:

$$\begin{aligned} \dot{V}_o = & (\mathbf{K}_{z_1} \mathbf{z}_1 + \mathbf{K}_{z_2} \mathbf{z}_2)^T (\mathbf{K}_{z_1} \dot{\mathbf{z}}_1 + \mathbf{K}_{z_2} (\mathbf{f} - \dot{\mathbf{x}}_{2d})) \\ & + \boldsymbol{\eta}^T \dot{\boldsymbol{\eta}} + \tilde{\boldsymbol{\theta}}_a^T \Gamma_{\theta a}^{-1} \dot{\tilde{\boldsymbol{\theta}}}_a + (\boldsymbol{\zeta} - \hat{\mathbf{d}}_T)^T \boldsymbol{\varepsilon}_\zeta (\dot{\boldsymbol{\zeta}} - \dot{\hat{\mathbf{d}}}_T) \\ & + (\mathbf{d}_T - \hat{\mathbf{d}}_T)^T \Gamma_{d_T}^{-1} (\dot{\mathbf{d}}_T - \dot{\hat{\mathbf{d}}}_T), \end{aligned} \quad (49)$$

where

$$\mathbf{f} = g\mathbf{e}_3 - \mathbf{I}_B \mathbf{R}^B \mathbf{v}_M \hat{\boldsymbol{\theta}}_a + \mathbf{I}_B \mathbf{R}^B \mathbf{v}_M \tilde{\boldsymbol{\theta}}_a + \mathbf{u}_{io} + \Delta \mathbf{u}_t + \mathbf{d}_T. \quad (50)$$

According to (5) and the inequality

$$-\tilde{\boldsymbol{\theta}}_a^T \dot{\tilde{\boldsymbol{\theta}}}_a \leq -\frac{\tilde{\boldsymbol{\theta}}_a^T \tilde{\boldsymbol{\theta}}_a}{2} + \frac{\boldsymbol{\theta}_a^T \boldsymbol{\theta}_a}{2}, \quad (51)$$

the term $-(\tilde{\boldsymbol{\theta}}_a^T \boldsymbol{\beta}_{\theta a} \tilde{\boldsymbol{\theta}}_a)/2 + ((\boldsymbol{\theta}_a^T \boldsymbol{\beta}_{\theta a} \boldsymbol{\theta}_a)/2)$ can be deduced after substituting $\tilde{\boldsymbol{\theta}}_a^T \Gamma_{\theta a}^{-1} \dot{\tilde{\boldsymbol{\theta}}}_a$ in (49).

When decomposing $\mathbf{d}_T - \hat{\mathbf{d}}_T$ into $\mathbf{d}_T - \mathbf{d}_{temp}$ and $\mathbf{d}_{temp} - \hat{\mathbf{d}}_T$ and conventionally magnifying the right side of (49), the intractable term $|\mathbf{d}_{tempj} - \hat{\mathbf{d}}_{Tj}| \Gamma_{d_Tj}^{-1} \dot{\hat{\mathbf{d}}}_{Tj}$ appears, where $j = x, y, z$. Recalling (9), we introduce the following inequation to substitute this term with a manageable one. For $\forall \varepsilon > 0$, and $\forall \gamma \in R$

$$0 \leq |\gamma| - \gamma \tanh\left(\frac{\gamma}{\varepsilon}\right) \leq k_p \varepsilon, \quad (52)$$

where k_p is a constant satisfying $k_p = e^{-(k_p+1)}$, whose approximation is chosen as 0.2758, which also meets the inequation (52). Therefore, there exists the following inequality:

$$|\mathbf{d}_{tempj} - \hat{\mathbf{d}}_{Tj}| \leq k_p \varepsilon_{\tilde{d}} + (\mathbf{d}_{tempj} - \hat{\mathbf{d}}_{Tj}) \tanh\left(\frac{\mathbf{d}_{tempj} - \hat{\mathbf{d}}_{Tj}}{\varepsilon_{\tilde{d}}}\right), \quad (53)$$

which facilitates the aforementioned substitution and the subsequent cancellation.

According to Chapter 4 in [31], regarding $g\mathbf{e}_3 + \mathbf{u}_t + \mathbf{d}_T$ as the input of the system (2), then due to the existence of the damping term, the system ${}^B\mathbf{v}(\mathbf{u}_t, \mathbf{d}_T)$ is input-to-state stable, implying that ${}^B\mathbf{v}$ is uniformly ultimately bounded with bounded \mathbf{u}_t and \mathbf{d}_T . Therefore, based on Assumptions 2 and 4 and the above analysis, there exist positive constants $C_{\theta a}$, $C_{k\varepsilon}$ and C_{d_T} satisfying

$$\begin{aligned} C_{\theta a} & \geq \|\tilde{\boldsymbol{\theta}}_a^T {}^B\mathbf{v}_M {}^B\mathbf{I} \mathbf{R} \Gamma_{d_T}^{-1} \boldsymbol{\sigma}_{d_T}\|, \\ C_{k\varepsilon} & \geq \|k_p \boldsymbol{\varepsilon}_\zeta^T \Gamma_{d_T}^{-1} (\mathbf{d}_T - \hat{\mathbf{d}}_T)\|, \\ C_{d_T} & \geq \|(\boldsymbol{\zeta} - \hat{\mathbf{d}}_T)^T \mathbf{K}_\zeta \dot{\hat{\mathbf{d}}}_T\|. \end{aligned} \quad (54)$$

For clarity, we perform the substitutions and transformations of the derivative (49) in two steps. Firstly, based on the proposed update laws (5)–(10) and the control law (3), also using (53) and (54), we have

$$\begin{aligned} \dot{V}_o \leq & -(\mathbf{K}_{z_1} \mathbf{z}_1 + \mathbf{K}_{z_2} \mathbf{z}_2)^T \mathbf{K}_{z_2} (\mathbf{K}_{z_1} \mathbf{z}_1 + \mathbf{K}_{z_2} \mathbf{z}_2) + \boldsymbol{\eta}^T \dot{\boldsymbol{\eta}} \\ & + (\mathbf{K}_{z_1} \mathbf{z}_1 + \mathbf{K}_{z_2} \mathbf{z}_2)^T \mathbf{K}_{z_2} (\Delta \mathbf{u} - \boldsymbol{\eta}) \\ & - \tilde{\boldsymbol{\theta}}_a^T (\boldsymbol{\beta}_{\theta a} - {}^B\mathbf{v}_M {}^B\mathbf{I} \mathbf{R} \mathbf{K}_{d_T} {}^B\mathbf{I} \mathbf{R} {}^B\mathbf{v}_M) \tilde{\boldsymbol{\theta}}_a \\ & - (\boldsymbol{\zeta} - \hat{\mathbf{d}}_T)^T \mathbf{K}_\zeta (\boldsymbol{\zeta} - \hat{\mathbf{d}}_T) - (\mathbf{d}_T - \hat{\mathbf{d}}_T)^T \mathbf{K}_{d_T} (\mathbf{d}_T - \hat{\mathbf{d}}_T) \\ & + \boldsymbol{\theta}_a^T \boldsymbol{\beta}_{\theta a} \boldsymbol{\theta}_a + C_{\theta a} + C_{k\varepsilon} + C_{d_T}. \end{aligned} \quad (55)$$

The second step considers the update law of $\boldsymbol{\eta}$. Using the update law given in (11), the derivative becomes

$$\begin{aligned} \dot{V}_o \leq & -(\mathbf{K}_{z_1} \mathbf{z}_1 + \mathbf{K}_{z_2} \mathbf{z}_2)^T \mathbf{K}_{z_2} (\mathbf{K}_{z_1} \mathbf{z}_1 + \mathbf{K}_{z_2} \mathbf{z}_2) - \boldsymbol{\eta}^T \mathbf{K}_\eta \boldsymbol{\eta} \\ & - \tilde{\boldsymbol{\theta}}_a^T (\boldsymbol{\beta}_{\theta a} - {}^B\mathbf{v}_M {}^B\mathbf{I} \mathbf{R} \mathbf{K}_{d_T} {}^B\mathbf{I} \mathbf{R} {}^B\mathbf{v}_M) \tilde{\boldsymbol{\theta}}_a \\ & - (\boldsymbol{\zeta} - \hat{\mathbf{d}}_T)^T \mathbf{K}_\zeta (\boldsymbol{\zeta} - \hat{\mathbf{d}}_T) - (\mathbf{d}_T - \hat{\mathbf{d}}_T)^T \mathbf{K}_{d_T} (\mathbf{d}_T - \hat{\mathbf{d}}_T) \\ & + \boldsymbol{\theta}_a^T \boldsymbol{\beta}_{\theta a} \boldsymbol{\theta}_a + C_{\theta a} + C_{k\varepsilon} + C_{d_T}, \end{aligned} \quad (56)$$

when $\|\boldsymbol{\eta}\| > \sigma_\eta$. In addition, with ${}^B\mathbf{v}$ bounded, also based on Assumption 2, the situation $\|\boldsymbol{\eta}\| \leq \sigma_\eta$ indicates that the position tracking error is bounded. Once Assumptions 2–4 are fulfilled, there exists a positive constant C_o satisfying

$$C_o \geq \boldsymbol{\theta}_a^T \boldsymbol{\beta}_{\theta a} \boldsymbol{\theta}_a + C_{\theta a} + C_{k\varepsilon} + C_{d_T}. \quad (57)$$

On the other hand, we select the positive constant k_{V_o} such that

$$0 < k_{V_o} \leq \min(K_{z_2j}, K_{\eta j}, \beta_{\theta aj} - V_{mj}, K_{\tilde{d}}, K_{d_Tj}), \quad (58)$$

with $V_m = {}^B\mathbf{v}_M {}^B\mathbf{I} \mathbf{R} \mathbf{K}_{d_T} {}^B\mathbf{I} \mathbf{R} {}^B\mathbf{v}_M$ and $j = x, y, z$, meanwhile $\beta_{\theta aj}$ should be set sufficiently large so that $\beta_{\theta aj} - V_{mj}$ are all positive for each j .

According to the previous analysis, we obtain the following inequation:

$$\dot{V}_o \leq -2k_{V_o}V_o + C_o, \quad (59)$$

which states that

$$V_o(t) \leq V_{o0} e^{-2k_{V_o}t} + \frac{C_o}{2k_{V_o}}(1 - e^{-2k_{V_o}t}), \quad (60)$$

where V_{o0} refers to the initial condition, and $C_o/(2k_{V_o})$ indicates the final convergence value. Therefore, $\lim_{t \rightarrow \infty} V_o(t) \leq (C_o/(2k_{V_o}))$. Since $V_o \in \mathcal{L}_\infty$, we have $(K_{z_1}z_1 + K_{z_2}z_2) \in \mathcal{L}_\infty$, further, $z_1 \in \mathcal{L}_\infty$ and $z_2 \in \mathcal{L}_\infty$, due to the relationship of $\dot{z}_1 = z_2$. Moreover, d_{Tj} , η and $(d_T - \hat{d}_T)$ are bounded, we know $\hat{d}_T \in \mathcal{L}_\infty$, then $(\zeta - \hat{d}_T) \in \mathcal{L}_\infty$. As a result, $\zeta \in \mathcal{L}_\infty$ and $u_o \in \mathcal{L}_\infty$, implying that Δu is bounded. Hence, we conclude that the parameters' update laws are also bounded. Provided that the assumptions and prerequisites of the averaging method are not violated, the bounds can be made arbitrarily small by tuning the controller gains. \square

5 Simulation results and analysis

Simulations are carried out in order to verify the validity of the proposed controller. According to the FMAV in [3], we set the system parameters as $J = \text{diag}(0.03, 0.03, 0.02) \text{ kg m}^2$, $m = 0.5 \text{ kg}$, $\theta_a = [1 \ 1 \ 0.4]^T \text{ s}^{-1}$ and $\theta_{ra} = [1 \ 1 \ 0.5]^T \text{ s}^{-1}$. The main controller gains are chosen as $K_{z_1} = \text{diag}(4, 4, 4)$, $K_{z_2} = \text{diag}(3, 3, 3)$, $k_q = 200$, $K_4 = \text{diag}(1, 1, 1)$, $\sigma_\eta = \sigma_{\eta_t} = \delta_a = 0.1$, $\delta_{m0} = 0.01$. The bounds of the estimated parameters are chosen as $\theta_{ai} \in (0.01, 2]$, $\theta_{rai} \in (0.25, 2.5]$, $\theta_{ra \times i} \in (-1, 1)$, for $i = x, y, z$. The way of tuning controller gains follows a basic guideline that the quaternion filter and the inner loop controller performs much faster than the outer loop one. Yet, the specific choice for the control gains depends on the performance of the control. In order to prevent dramatic change of control inputs, excessively small σ_η , σ_{η_t} , δ_a , δ_{m0} are not recommended. However, smaller bounds usually generate smaller tracking errors. As a result, this is a tradeoff between robustness and accuracy.

Case 1 (Tracking sinusoidal trajectory): Here we select the original desired trajectory as $x_d = 1 \sin(t)$, $y_d = 1 \sin(t)$, $z_d = 2.5 \sin(t)$, $\psi_d = \pi$. A second-order filter is used to smooth the desired trajectory. In order to show the input constraint phenomenon, their feasible regions are set within a narrow scope as $\|u\| \in (8, 12)$, $\tau_x \in (-10, 10)$, $\tau_y \in (-10, 10)$, $\tau_z \in (-15, 15)$. In order to validate the robustness of the controller, we apply zero mean random noises to the acceleration layer of rotation and translation, whose variances are 0.02 and 0.2, respectively. The obtained simulation results are shown in Figs. 3 and 4.

From Figs. 3 and 4, it can be seen that the thrust force reaches its upper bound repeatedly, and the X, Y position errors increase at the same time. However, the system's tracking errors remain bounded, as indicated by the simulation results. The system meets no singularity, even though the yaw angle reaches 180 degrees.

Case 2 (Tracking linear trajectory): Desired trajectories of ramp functions are tested in this case. The controller parameters remain the same as those in Case 1. We choose the original desired trajectory as $x_d = 3t$, $y_d = 3t$, $z_d = 3t$, $\psi_d = (\pi/2)t$. Based on the simulation results shown in Figs. 5 and 6, we conclude that the vehicle is capable to track the ramp function with the proposed controller. It can be also seen from the simulation results that saturation occurs for the thrust force, yet its influences are tolerable due to the specific design of the control law. Moreover, although the noise has more significant influences on the torques than on the thrust force, the torques remain bounded and the tracking error of the yaw angle keeps relatively small.

Case 3 (Robustness test): To examine the capability of handling large angular error, Case 2 is re-implemented with a new initial

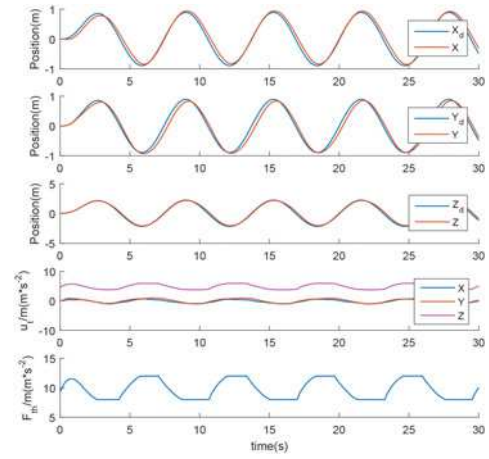


Fig. 3 Trajectory of translational position, corresponding desired force in three directions and constrained thrust input in Case 1

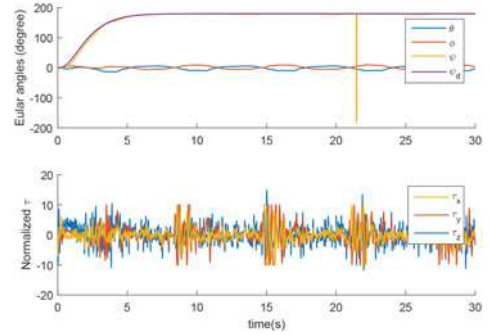


Fig. 4 Trajectory of rotational position and corresponding constrained normalised torques in Case 1

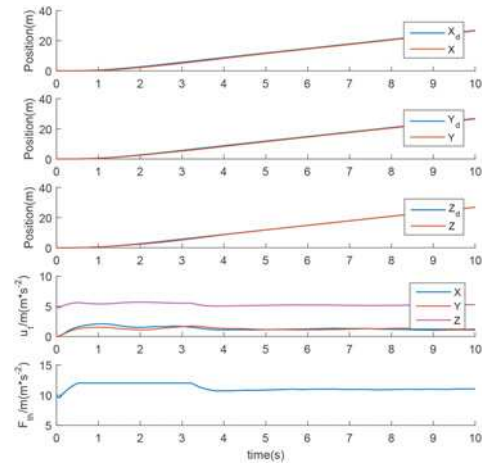


Fig. 5 Trajectory of translational position, corresponding desired force in three directions and constrained thrust input in Case 2

condition that the vehicle is upside down. After analysing the results shown in Fig. 7, it can be drawn that the angular controller remains effective even when the angular error is relatively large. The system gradually converges to the similar trajectory as Case 2.

It can be extracted from the simulation results that the fast oscillating instant thrust force is successfully approximated by a changing sinusoidal function with the form of $F_{ins} = k_F \omega_m^2 \sin(\theta_p) + k_F \omega_m^2$, $\dot{\theta}_p = \omega_m$, whose average value is modulated as F_{th} . Using quaternion-based hybrid attitude tracking

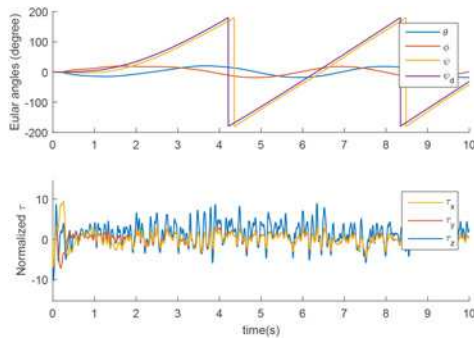


Fig. 6 Trajectory of rotational position and corresponding constrained normalised toques in Case 2

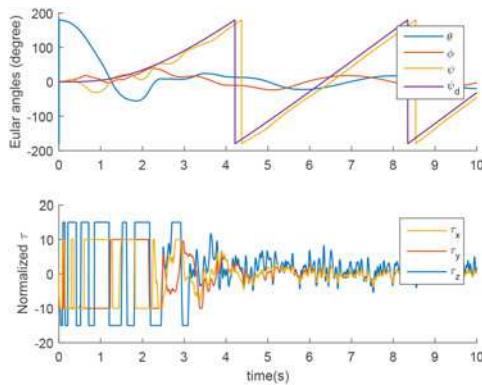


Fig. 7 Trajectory of rotational position and corresponding constrained normalised toques in Case 3

controller, the system faces no singularity when ψ approaches π , and still performs well even with the presence of large initial errors. Both the position and attitude tracking errors are successfully kept within acceptable bounds even under the interference of random noises. Although the FMAV model in [13] is not identical with the one studied in this paper, it can be concluded from [23] that the control strategy of [13] degrades quickly due to the chattering problem when the attitude error is relatively large. Input constrained tracking control of FMAV was also discussed in [25], compared with their method, our proposed control strategy yields smoother tracking trajectories, which means the proposed control law is more robust and suitable for practical applications. In general, the simulation results reveal some peculiar advantages over existed methods as mentioned above.

6 Conclusions

This paper introduces a systematic method to solve the tracking control problem of flapping wing vehicle. Based on the idea that the averaging estimation error and the drift of the averaged system can be regarded as the disturbance, we propose an adaptive tracking controller with input constraint, which manages to keep the tracking error sufficiently small. The new-designed quaternion-based attitude tracking controller is robust for tolerating disturbances within reasonable limits. The inner loop controller remains effective even when the initial angle error is set as 180° . By neglecting the oscillating signals, the proposed strategy also shows its non-trivial capability in generating smoothly varied control inputs, which benefits to wear reducing. However, some problems remain unsolved. When the approximation error of every cycle becomes larger, i.e. the flapping frequency is exceedingly low, the averaging method might fail, then, there is no guarantee for the performance of the proposed controller. In the future, we

will implement hardware experiments, and explore more specific properties of flapping wing micro vehicle dynamics. The rigorous analysis of the averaging effects will also be considered in the forthcoming studies.

7 Acknowledgments

This work was supported by National Natural Science Foundation of China under grant no. 61633012, and in part by the Natural Science Foundation of Tianjin under grant no. 16JCZDJC30300.

8 References

- [1] Shyy, W., Kang, C., Chirarattananon, P., *et al.*: 'Aerodynamics, sensing and control of insect-scale flapping-wing flight', *Proc. R. Soc. A*, 2016, **472**, (2186), doi: 10.1098/rspa.2015.0712
- [2] Shyy, W., Aono, H., Chimakurthi, S.K., *et al.*: 'Recent progress in flapping wing aerodynamics and aeroelasticity', *Prog. Aerosp. Sci.*, 2010, **46**, (7), pp. 284–327
- [3] Zdunich, P., Bilyk, D., MacMaster, M., *et al.*: 'Development and testing of the mentor flapping-wing micro air vehicle', *J. Aircr.*, 2007, **44**, (5), pp. 1701–1711
- [4] de Croon, G.C.H.E., de Clercq, K.M.E., Ruijsink, R., *et al.*: 'Design, aerodynamics, and vision-based control of the DelFly', *Int. J. Micro Air Veh.*, 2009, **1**, (2), pp. 71–97
- [5] Keennon, M., Klingebiel, K., Won, H., *et al.*: 'Development of the nano hummingbird: a tailless flapping wing micro air vehicle'. Proc. AIAA Aerospace Sciences Meeting, Nashville, USA, January 2012
- [6] Wood, R.J.: 'The first takeoff of a biologically inspired at-scale robotic insect', *IEEE Trans. Robot.*, 2008, **24**, (2), pp. 341–347
- [7] Prez-Arancibia, N.O., Duhamel, P.E.J., Ma, K.Y., *et al.*: 'Model-free control of a flapping-wing flying microrobot'. Proc. 16th Int. Conf. Advanced Robotics (ICAR), Montevideo, Uruguay, 25–29 November 2013
- [8] Zhang, J., Cheng, B., Yao, B.: 'Adaptive robust wing trajectory control and force generation of flapping wing MAV'. Proc. IEEE Int. Conf. on Robotics and Automation (ICRA), Seattle, WA, USA, 26–30 May 2015
- [9] Chirarattananon, P., Ma, K.Y., Wood, R.J.: 'Adaptive control of a millimeter-scale flapping-wing robot', *Bioinspir. Biomimetics*, 2014, **9**, (2), doi: 10.1088/1748-3182/9/2/025004
- [10] Taha, H.E., Woolsey, C.A., Hajj, M.R.: 'A geometric control approach for optimum maneuverability of flapping wing MAVs near hover'. Proc. American Control Conf. (ACC), Washington, USA, 17–19 June 2013
- [11] Taha, H.E., Hajj, M.R., Nayfeh, A.H.: 'Flight dynamics and control of flapping-wing MAVs: a review', *Nonlinear Dyn.*, 2012, **70**, (2), pp. 907–939
- [12] Lin, S.H., Hsiao, F.Y., Chen, C.L., *et al.*: 'Altitude control of flapping-wing MAV using vision-based navigation'. Proc. American Control Conf. (ACC), Baltimore, MD, USA, 21–26 June 2010
- [13] Banazadeh, A., Taymourtash, N.: 'Adaptive attitude and position control of an insect-like flapping wing air vehicle', *Nonlinear Dyn.*, 2016, **85**, (1), pp. 47–66
- [14] Chirarattananon, P., Ma, K.Y., Wood, R.J.: 'Adaptive control for takeoff, hovering, and landing of a robotic fly'. Proc. Int. Conf. Intelligent Robots and Systems, Tokyo, Japan, 3–7 November 2013
- [15] Khan, Z.A., Agrawal, S.K.: 'Control of longitudinal flight dynamics of a flapping-wing micro air vehicle using time-averaged model and differential flatness based controller'. Proc. American Control Conf. (ACC), New York, USA, 9–13 July 2007
- [16] Taha, H.E., Tahmasian, S., Woolsey, C.A., *et al.*: 'The need for higher-order averaging in the stability analysis of hovering, flapping-wing flight', *Bioinspir. Biomimetics*, 2015, **10**, (1), doi: 10.1088/1748-3190/10/1/016002
- [17] Vela, P.A.: 'Averaging and control of nonlinear systems'. Ph.D. dissertation, California Institute of Technology, 2003
- [18] Sanders, J.A., Verhulst, F., Murdock, J.A.: 'Averaging methods in nonlinear dynamical systems' (Springer, New York, 2007)
- [19] Schenato, L.: 'Analysis and control of flapping flight: from biological to robotic insects'. Ph.D. dissertation, University of California, Berkeley, 2003
- [20] Cao, N., Lynch, A.F.: 'Inner-outer loop control for quadrotor UAVs with input and state constraints', *IEEE Trans. Control Syst. Technol.*, 2016, **24**, (5), pp. 1797–1804
- [21] Chen, M., Ge, S.S., Ren, B.: 'Adaptive tracking control of uncertain MIMO nonlinear systems with input constraints', *Automatica*, 2011, **47**, (3), pp. 452–465
- [22] Xian, B., Diao, C., Zhao, B., *et al.*: 'Nonlinear robust output feedback tracking control of a quadrotor UAV using quaternion representation', *Nonlinear Dyn.*, 2015, **79**, (4), pp. 2735–2752
- [23] Mayhew, C.G., Sanfelice, R.G., Teel, A.R.: 'Quaternion-based hybrid control for robust global attitude tracking', *IEEE Trans. Autom. Control*, 2011, **56**, (11), pp. 2555–2566
- [24] Deng, X., Schenato, L., Sastry, S.S.: 'Flapping flight for biomimetic robotic insects: part II-flight control design', *IEEE Trans. Robot.*, 2006, **22**, (4), pp. 776–788
- [25] Rifai, H., Marchand, N., Poulin, G.: 'Path tracking control of a flapping unmanned air vehicle (UAV)'. Proc. 17th IFAC World Congress, Seoul, Korea, July 2008, pp. 5359–5364

- [26] Wen, C., Zhou, J., Liu, Z., *et al.*: 'Robust adaptive control of uncertain nonlinear systems in the presence of input saturation and external disturbance', *IEEE Trans. Autom. Control*, 2011, **56**, (7), pp. 1672–1678
- [27] Farrell, J.A., Polycarpou, M., Sharma, M., *et al.*: 'Command filtered backstepping', *IEEE Trans. Autom. Control*, 2009, **54**, (6), pp. 1391–1395
- [28] Sanfelice, R.G., Goebel, R., Teel, A.R.: 'Invariance principles for hybrid systems with connections to detectability and asymptotic stability', *IEEE Trans. Autom. Control*, 2007, **52**, (12), pp. 2282–2297
- [29] Zhao, B., Xian, B., Zhang, Y.: 'Nonlinear robust adaptive tracking control of a quadrotor UAV via immersion and invariance methodology', *IEEE Trans. Ind. Electron.*, 2015, **62**, (5), pp. 2891–2902
- [30] Tran, T.T., Ge, S.S., He, W.: 'Adaptive control of a quadrotor aerial vehicle with input constraints and uncertain parameters', *Int. J. Control*, 2017, **91**, (5), pp. 1140–1160
- [31] Khalil, H.K.: 'Nonlinear systems' (Prentice Hall, New Jersey, 2002, 3rd edn.)